On THz cyclotron resonance continuous wave lasers in graphene in crossed E, H fields at $T = 300$ K

© A.A. Andronov, V.I. Pozdniakova

Institute of Physics of Microstructures, Russian Academy of Sciences,
603950 Nizhny Novgorod, Russia

E-mail: andron@ipmras.ru

Received April 18, 2022
Revised January 31, 2023
Accepted January 31, 2023

In framework of classical consideration of electron trajectories in crossed E, H fields and conductivity of electron system on cyclotron resonance in single layer graphene possibility to achieve THz cyclotron lasing in hexagonal boron nitride–single layer graphene sandwiches is discussed. By simplified consideration with known data on scattering rate in the sandwiches it is demonstrated that the CW laser action can be achieved in high quality sandwiches at room temperature at frequencies above about 0.5−1 THz in magnetic field above 5000−10000 Gauss. Short discussions of Landau level quantization in crossed fields, amplification on cyclotron harmonics and cyclotron amplification at low temperatures are given.

Keywords: graphene, cyclotron resonance, THz amplification, Landau level population inversion.

DOI: 10.21883/SC.2023.01.55617.3548

1. Introduction

The possibility of cyclotron–resonance (CR) amplification in crossed E, H fields in semiconductors due to the accumulation of electrons on closed trajectories in momentum space with an electron energy lower than the energy of an optical phonon, wherein there is only weak elastic scattering due to the low temperature of the semiconductor, was first noted in [1]. Then a similar possibility was indicated for light holes in p-Ge [2]. A THz laser based on this mechanism was first demonstrated in [3]. Then many scientists of the world developed this work (see, for example, [4,5]). Although the lasers demonstrated a very broad frequency tuning (by 2−3 times) with change of E and H, they were not widely used, since they operated in pulsed mode and with a liquid helium cooling. At the same time, CW continuous frequency tunable sources of THz radiation, even those operating with liquid helium, could be extremely important for a number of applications, including atmospheric monitoring research systems on Earth and in space, using circuits with THz heterodynes. Such a THz radiation source operating at room temperature could provide the basis for the broadest application.

High mobility boron nitride (hBN)-graphene sandwiches have been demonstrated in recent years. The use of boron nitride for the substrate (and „overlay“) during the graphene growth and the creation of sandwiches is due to the fact that the parameters of its lattice are very close to the parameters of the graphene lattice. As a result, the quality and mobility in sandwiches is an order of magnitude higher than, say, in graphene on SiO_2. At the same time, sandwich — is already such a system that can be used to create devices.

In particular, the THz radiation amplification in a sandwich with single-layer graphene (SLG) with a system of gate plasmons at $T = 300$ K and in continuous mode with a very broad frequency tuning by an electric field was published in [6]. As a matter of fact, this paper stimulated this study together with a proposal to conduct it from Eric Gornik (Vienna). In addition, a THz detector on gate plasmons in a sandwich with dual-layer graphene (DLG) [7] and a THz detector on plasmons near the second harmonic of the CR in a sandwich with a SLG [8] were created.

Graphene — is a semiconductor system with a zero band gap and a linear („Dirac“) law of dispersion of electrons and holes with sufficiently low energies. Boron nitride (hBN)--graphene sandwiches are not doped for obtaining high quality and mobility of carriers, and the concentration of electrons or holes is created by the voltage at the gate fabricated on the outer surface of the sandwich, as, say, in paper [6]. As demonstrated, for example, in the work [6], the concentration does not change with high voltage (> 6 kV/cm), producing current in graphene. This has also been observed in other studies of the current in graphene in strong electric fields with an electron concentration determined by the gate voltage (see, for example, [9,10]). In particular, the transport in the single-layer graphene in strong fields was simulated in the paper [10] without any consideration of breakdown or tunneling, which showed complete coincidence with observations of such transport in the SLG. The breakdown in the SLG was observed only in doped graphene with high current and very strong electric field [11,12]. In particular, the paper [12] covers the measurements of the electron concentration that is produced in doped graphene of the p-type when a strong THz field is applied. It was found that any noticeable additional concentration of electrons is produced in the fields > 100 kV/cm. This value of the fields is more than an order of magnitude higher than the

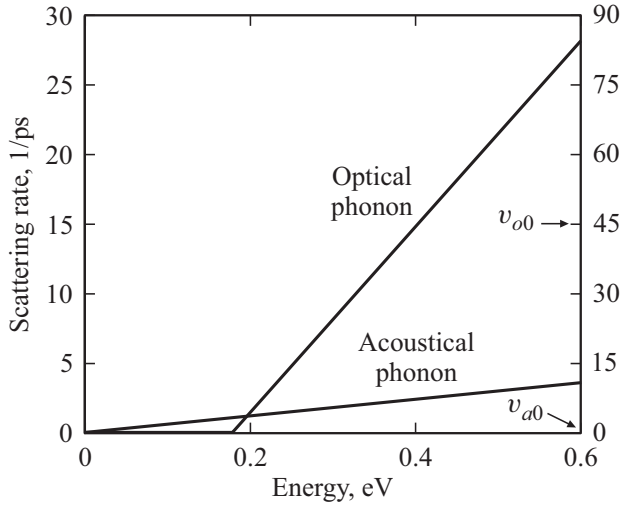

Figure 1. Scattering rates in the SLG at $T = 300$ K. The numbers on the left axis are adapted from the calculations of [15]; the scattering rate on optical phonons — is the sum of the scattering rates on intervalley and intravalley optical phonons. The numbers on the right axis — are simply tripled values of the left axis to (as was done in [13]) take into account the scattering on phonons in *h*B*N* in sandwiches. Such a tripling seems justified, and for acoustic phonons is confirmed by measurements of mobility and streaming threshold in sandwiches at $T = 300$ K [6] (see [13]). The dependence of scattering rates on energy — there are straight lines due to the Dirac dependence of electron energy on the momentum and electron scattering by at the deformation potential.

values of the fields discussed in this paper. In addition, this value is close to the estimate of the tunneling field in the SLG with an electron energy comparable to the energy of an optical phonon. Therefore, we will not discuss further the role of breakdown or tunneling in the effects under consideration.

In work [13] we explained the results of [6] based on the dispersion and negative THz conductivity of hot electrons in a sandwich in an electric field as a result of electron bunching at a transit time flight resonance up to the energy of an optical phonon during electron streaming. Only a change of the sign of the real part of the permittivity response in case of a transit time flight resonance can explain the disappearance of the resonance on the gate plasmons in the interval of electric fields, observed in the paper [6]. Such effects of electron amplification of microwave radiation during streaming were also discussed in [1] and were demonstrated in *n*-InP [14] with a wide tuning of the microwave frequency by an electric field.

All these results indicate that there is a real possibility to implement a continuous THz laser on the CR in crossed E, H fields at high temperatures, since the energy of the optical phonon in the sandwiches is ~ 2000 K. In addition, the ratio ν_{o0}/ν_{a0} of characteristic scattering rates on optical ν_{o0} and acoustic ν_{a0} phonons is about 15 at $T = 300$ K in the SLG and should be significantly larger in the sandwich (Fig. 1) This value determines the possibility of CR amplification in the crossed E, H fields.

This motivational work is aimed at attracting researchers to carry out experimental studies of THz properties of sandwiches with SLG in strong E, H fields, developing, clarifying and complementing the papers [6,13].

2. Trajectories and electron distribution function in graphene in E, H fields

The Brillouin zone of graphene consists of 6 „valleys“, K and K', with different pseudo-spin states, with centers located at the boundary of the zone, wherein only one third of each valley is inside the first Brillouin zone. The valleys, though ones at along the boundary, have different pseudospin states, and otherwise are the same — have the same isotropic Dirac electron spectrum. Since we have three valleys K and three valleys K' with one third in the Brillouin zone, we can assume that we have two complete valleys with different pseudospins, so that a twofold degeneracy of electronic states is obtained taking into account the electron spin. There can be both intravalley and intervalley scatterings in case of scattering on phonons. When estimating the scattering values in sandwiches, we will focus on the paper of [15], where the scattering rates on phonons and electron-electron scattering are calculated at $T = 300$ K (cf. Fig. 1) just in graphene. Calculations show that the intervalley scattering makes the main contribution in case of optical phonons. Figure 1 shows the sum of intravalley and intervalley scatterings for scattering rate on optical phonons. But we are interested in the scattering rates in sandwiches — their calculations are missing. In sandwich, as in paper [13], due to the lack of choice (there are no calculations or measurements), we simply triple the scattering rates on phonons (Fig. 1) compared with the rates in graphene, bearing in mind the proximity of the parameters of the boron nitride and graphene lattices. Electron-electron scattering in sandwiches should be less than in a separate layer of the SLG, due to additional screening of the Coulomb field by layers of boron nitride. But further, for evaluation, we will assume that this rate do not change in the sandwich and we can use the data of [15]. This scattering is an important parameter that determines the maximum electron concentration at which the CR amplification is still possible.

As in *p*-Ge, graphene has a strong emission of optical phonons by electrons, and there is a nonequidistance of Landau levels. This all determines the inversion of the populations of the Landau levels and the negative conductivity at CR.

Next, we discuss the above problems based on the consideration of electron trajectories and conductivity on the CR in the framework of classical concepts, with virtually one exception, without considering Landau levels. In addition, we use a simple analytical approach to determine

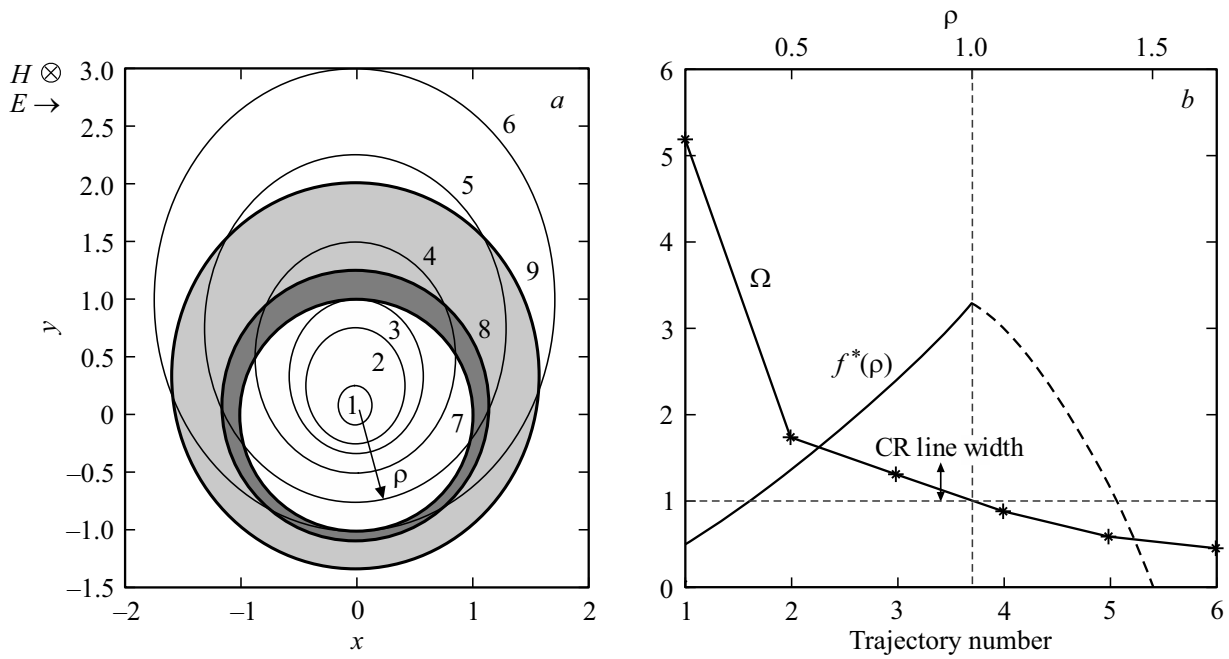

Figure 2. *a* — electronic trajectories in the SLG in crossed E, H fields with $D = cE/HV_F = 0.5$; the trajectories (*1–6*), the energy of the optical phonon (*7*) and the upper limits of the emission of optical phonons on the trajectories *1*(*8*) and *3* (*9*) are shown; the areas from which optical phonons are emitted to these trajectories are marked; ρ — the radius of the trajectories. *b* — cyclotron frequencies on trajectories and the electron distribution function on them as a function of their radius ρ. The width of the CR line necessary for the negative conductivity on the CR is also marked.

the electron trajectory distribution function. Figure 2 shows the trajectories and their cyclotron frequencies in the SLG in crossed fields for the „Dirac" electron zone with electron energy $\varepsilon = V_F p$, V_F — Fermi velocity, p — electron momentum with components p_x, p_y, $E = E_x$ and $H = H_z$ in dimensionless variables $\mathbf{r} = \mathbf{p}/p_0$, $\tau = \omega_c t$, $\omega_c = eH/mc$, $m = p_0/V_F$, $\varepsilon_0 = V_F p_0 = \hbar\omega_0$ — the energy of the optical phonon with $D = cE/HV_F = 0.5$. The trajectories — are ellipses $r - Dy = \text{const}$ (for $D < 1$). The estimated electron distribution function $f^*(\rho)$ is also presented, averaged along the trajectory (by the angle of the trajectory, approximated by a circle, with a radius of ρ). In the inversion region in the distribution $(df^*(\rho)/d\rho > 0)$, the approximate value is $f^* = A(\rho^2 + 2\rho)$, where $A \approx 12/11$ with neglect of the contribution of the trajectories entering the region $r > 1 (\varepsilon > \varepsilon_0)$, and putting $\int \rho f^*(\rho) d\rho = 1$. The expression for f^* is based on formulas for the scattering rates in the SLG on optical ν_o $(\varepsilon > \hbar\omega_0)$ and acoustic $\nu_a (\varepsilon < \hbar\omega_0)$ phonons (Fig. 1):

$$\nu_o = (r-1)\nu_{o0}, \quad \nu_a = r\nu_{a0}, \tag{1}$$

where ν_{o0} and ν_{a0} are constants. When an optical phonon is emitted,p changes to p_0 (i.e., r by 1). Then if an electron emits an optical phonon from $r = r_i > 1$ with a rate $\nu_o = (r_i - 1)\nu_{o0}$, it turns into a state with $r_f = (r_i - 1)$ in the region $r < 1$, where the scattering rate $\nu_a = r_f \nu_{a0} = (r_i - 1)\nu_{a0}$. As a result, the relation ν_o/ν_a for any r_i — is $\nu_{o0}/\nu_{a0} = \text{const}$. We estimated the value of $f^*(\rho)$, assuming that the frequency of CR is $\omega_c \gg \nu_{o0}$. In this case, the population of the trajectories entering the area $\varepsilon > \varepsilon_0$ can be considered approximately the same. Now, since the ratio ν_o/ν_a of the rate of arrival to the rate of outgoing from the trajectories at $r < 1$ is constant, the population of the trajectories is proportional to the area on the plane p_x, p_y, from which optical phonons are emitted to one that or another trajectory (two examples are shown in Fig. 2). These regions are located above the energy of the optical phonon and below the upper boundary of the transitions to the trajectory. Most likely, this estimate also works for $\omega_c \approx \nu_o$.

3. The conductivity of electrons in graphene in E, H fields

When viewed classically in τ- approximation, the real part of the conductivity on the CR in an alternating field of circular polarization resonant with the rotation of electrons for the distribution function $f(p)$ along the radius of the trajectories p assumed to be circular is equal to

$$\text{Re}\,\sigma_c(\omega) = -\frac{e^2 N_S}{2} \int \frac{df}{dp} \frac{p^2}{m} \frac{\nu(p)}{(\omega - \omega_c(p))^2 + \nu^2(p)}\, dp. \tag{2}$$

Here $\nu(p) = 1/\tau$ — scattering rate, N_S — surface electron concentration and $\int p f\, dp = 1$. In limit $\nu(p) \to 0$,

$$\frac{\nu(p)}{(\omega - \omega_c(p))^2 + \nu^2(p)} \to \pi\delta(\omega - \omega_c(p)), \qquad (3)$$

$\delta(\omega - \omega_c(p))$ — δ-function. Then we obtain

$$\mathrm{Re}\,\sigma_c(\omega) = -\frac{e^2 N_S p^2}{2m} \frac{\pi}{|d\omega_c(p)/dp|} \frac{df}{dp} \qquad (4)$$

for $p = p^*$ from $\omega = \omega(p^*)$. This expression retains the form if you replace p with ρ and use $f^*(\rho)$. So, if $(df/dp)_{p^*} > 0$, then $\mathrm{Re}\,\sigma_c(\omega) < 0$. The condition under which the expression (4) would be fair is as follows: it is necessary that the response be local in p, as shown in Fig. 2. For this, it is necessary that the scattering rate (the width of the CR line) be less than the spread of the CR frequency in the area of population inversion. In Figure 2, this spread is about $0.5\omega_c$ for $\rho \approx 0.75$ (trajectory *3*), and it is necessary that $\nu(p) < 0.5\omega_c$ and for the expression (4) be true. This condition is the main one for the existence of $\mathrm{Re}\,\sigma_c(\omega) < 0$, since the condition $\omega_c \gg \nu_{o0}$, as mentioned above, is not critical.

From the point of view of describing the conductivity on the CR in the language of Landau levels, the expression (4) is the sum of transitions between many pairs of Landau levels, as a result, the scattering rate frequency ν falls out of the expression for conductivity (4), and with an increase in the cyclotron frequency ω_c, the number of these levels decreases, and the conductivity decreases, since in (4) ω_c in the denominator. On the other hand, the performed calculations allow within the framework of a quasi-classical description of Landau levels and their population, writing an expression for the conductivity in case of the transition between two Landau levels. Indeed, the population of the Landau level is determined by the total value of the classical cyclotron trajectory distribution function $f(p)$ for the electron energy between the two nearest Landau levels. In turn, the population difference of the nearest Landau levels Δn will be equal to the product of the derivative of the electron distribution function df/dp by the number of states Σ (area in p-space) in the area of trajectories between Landau levels: $\Delta n = \Sigma df/dp$. With our normalizing $f(p)$ (angle integrated), the value $\Sigma = p\Delta p$, where Δp — the change in the radius of the trajectory when the energy changes by $\hbar\omega_c$. As a result $\Sigma = p/V_\mathrm{F}\,\hbar\omega_c$ and instead of (2) we can (should) write for the transition between two Landau levels

$$\mathrm{Re}\,\sigma_c = -\frac{e^2 N_S p \Delta n}{2m} \frac{\nu}{(\omega_c - \omega)^2 - \nu^2}. \qquad (5)$$

If we rewrite Δn using the distribution function of $\rho - f^*(\rho) = f(p)/p_0^2$, we will obtain on the resonance $\omega_c = \omega$

$$\mathrm{Re}\,\sigma_c = -\frac{e^2 N_S \rho^2}{2m} \frac{df^*(\rho)}{d\rho} \frac{\omega_c/\omega_0}{\nu}. \qquad (6)$$

Formulas (4) and (6) thus refer to the two limiting cases of, respectively, relatively low and high cyclotron frequencies. Moreover, the latter case is more interesting for low temperatures, when in perfect sandwiches the scattering rate frequency ν can be less than the value at $T = 300\,\mathrm{K}$ by an order of magnitude [8], and it is natural to use superconducting magnets to obtain high cyclotron frequencies.

4. Estimates of the magnitude of negative conductivity in graphene in E, H fields

Now let's estimate the value of $\mathrm{Re}\,\sigma_c(\omega) < 0$ using the expression (4). We use the values from Fig. 1 for the scattering rates frequencies in the sandwich with SLG: $\nu_{a0} = 3 \cdot 10^{12}\,\mathrm{c}^{-1}$ and for $T = 300\,\mathrm{K}$. It is also important that in perfect sandwiches, the scattering rates frequency on acoustic phonons decreases with a decrease in temperature [8], expanding the frequency range for $\mathrm{Re}\,\sigma_c(\omega) < 0$. But here we consider only the case of $T = 300\,\mathrm{K}$. The main condition for $\mathrm{Re}\,\sigma_c(\omega) < 0$ — $\nu(p) < 0.5\omega_c$, and for $\nu(p)$ we should take the average value of $\nu_a(p) = \nu_{a0}\rho$ for $\rho < 1 - \nu_{a0}/2$. As a result, we obtain the condition for $\mathrm{Re}\,\sigma_c(\omega) < 0 \nu_{a0} < \omega_c$ or $\omega_c > 3 \cdot 10^{12}\,\mathrm{c}^{-1}$. Making the condition for $\mathrm{Re}\,\sigma_c(\omega) < 0$ stronger, we double the frequency to $\omega_c > 6 \cdot 10^{12}\,\mathrm{c}^{-1}$, or for a simple frequency $f_0 > 1\,\mathrm{THz}$. The frequency Ω in Figure 2 is normalized to the frequency $\omega_{c0} = eH/mc$, where $m = p_0/V_\mathrm{F} \approx 0.03m_0$. For such m $\omega_c \approx 6 \cdot 10^8\,\mathrm{H\,(Gs)}$ and for $\Omega = \omega_c/\omega_{c0} \approx 1$ with $\rho \approx 0.7$ $\omega_c \approx 6 \cdot 10^{12}\,\mathrm{c}^{-1}$ ($f_0 \approx 1\,\mathrm{THz}$) for $H \approx 10\,000\,\mathrm{Gs}$. A magnetic field of a couple tens of thousands Gs in a small volume ($1 \times 3 \times 3\,\mathrm{mm}^3$ for a small THz resonator placed between magnetic concentrators) can be obtained at $T = 300\,\mathrm{K}$ (or at $T = 78\,\mathrm{K}$). But superconducting magnets are needed for a broader upward frequency tuning. Thus, the value of $\mathrm{Re}\,\sigma_c(\omega) < 0$ of (4) for the given parameters is

$$|\mathrm{Re}\,\sigma_c(\omega)| = \frac{e^2 N_S p^2}{2m} \frac{\pi}{|d\omega_c(p)/dp|} \frac{df}{dp} \approx \frac{2e^2 N_S}{m\omega_c(p^*)}.$$

An important question is what value to take for N_S. The greater is its value, the greater is $|\mathrm{Re}\,\sigma_c(\omega)|$ and the easier it is to produce the laser radiation. But in the discussion above, we did not take into account electron-electron ($e-e$) scattering, which can suppress inversion. To avoid this, the rate of $e-e$ scattering should be less than the rate of acoustic scattering. In paper [15], the rate frequency of $e-e$ scattering in the degenerated gas was calculated when discussing the nonlinear conductivity of the SLG at $T = 300\,\mathrm{K}$. It was assumed that the scattering occurs on an equilibrium distribution function and, as one can be assumed, inside one valley. For having nothing of something better, we will use these calculations. For the electron energy less than the energy of the optical phonon, this frequency is $3 \cdot 10^{13}\,\mathrm{c}^{-1}$ for $N_S = 7.7 \cdot 10^{12}\,\mathrm{cm}^{-2}$. The

scattering rate is proportional to N_S. Therefore, in order for this rate to be less than the scattering rate on acoustic phonons ($1.5 \cdot 10^{12}\,c^{-1}$), it is necessary to divide N_S by 20, obtaining $N_S \approx 4 \cdot 10^{11}\,cm^{-2}$. But the calculations in [15] actually relate to a separate „valley" of SLG, since the intervalley $e-e$ scattering is small. There are, as noted above, two full valleys in the Brillouin SLG zone. Each of them contributes to the conductivity on the CR. Therefore, the total possible value of N_S in all valleys is $N_S \approx 10^{12}\,cm^{-2}$. The experiment should provide more accurate data. Note that in the paper [6], where, as we believe, electron streaming was observed (which is also suppressed by $e-e$ scattering), it persisted to N_S at least up to several units at $10^{12}\,cm^{-2}$. Of course, this is still a preliminary estimation. In addition, a strong magnetic field can change the rate frequency of $e-e$ scattering. An experiment is needed.

Estimated value $|\mathrm{Re}\,\sigma_c(\omega)|$ from (4) with $N_S = 10^{12}\,cm^{-2}$ for $f_0 = 1\,THz$ ($\omega_c(p^*) = 6 \cdot 10^{12}\,c^{-1}$): $|\mathrm{Re}\,\sigma_c(\omega)| \approx 2 \cdot 10^9$ cm/s. This is the surface conductivity that determines the surface current j_S in the electric field $\tilde{E}$ of the electromagnetic wave on this surface: $j_S = \mathrm{Re}\,\sigma_c(\omega)\tilde{E}$. This current, in turn, determines the jump in the magnetic field of the wave $\tilde{H} = (4\pi/c)j_S = (4\pi/c)\mathrm{Re}\,\sigma_c(\omega)\tilde{E} = 0.8\tilde{E}$ and the ratio $\tilde{E}/\tilde{H} = 1/0.8$ on the surface, demonstrating a sufficiently large effect of amplification of the electromagnetic wave and the possibility of its use in the CR a laser on the CR.

5. Conclusion

We have demonstrated that SLG sandwiches can be used to create CR lasers in crossed E, H fields at $T = 300\,K$ for THz frequencies above $0.5-1\,THz$. There is no doubt that such a laser can operate in continuous mode, since due to the presence of a magnetic field, the heating problems should be more gentle compared to observations of THz radiation amplification in continuous mode in a sandwich in the absence of a magnetic field [6] in an electric field $4-6\,kV/cm$ at $T = 300\,K$. In our case, to get the value considered above, $D = cE/HV_F = 0.5$ at $H = 10\,000\,Gs$ needs an electric field $\sim 5\,kV/cm$. Moreover, due to the ratio ν_{o0}/ν_{a0} is large, the bulk of the electrons are on trajectories at $\varepsilon < \varepsilon_0$, where the scattering rate frequency is small compared to the cyclotron frequency, and the main electric field is the Hall field. The dissipative electric field is significantly smaller than the Hall field, which reduces the dissipation compared to the case without a magnetic field discussed in [6].

A magnetic field greater than $H = 10\,000\,Gs$, is large enough for wide application at $T = 300\,K$. The reduction of the field can be achieved using trajectories with a smaller radius ρ, where the cyclotron mass is less (Fig. 2), or using the harmonics of cyclotron motion. Although the harmonics are small (their amplitudes are $\sim 0.2\rho$ in case of the second harmonic and $< 0.1\rho$ third harmonic), they are present in cyclotron oscillations. We would like to underline that the above analysis of the CR conductivity refers to a homogeneous THz field „fast" electromagnetic wave. At the same time, the response of the SLG in crossed fields to „slow" waves with a wavelength of the order of the cyclotron radius is also present on harmonics of cyclotron frequency and in the absence of harmonics in cyclotron motion. This was demonstrated in the study of THz photoconductivity in [8]. It is possible that some system with slow waves (for example, a system with gate plasmons, as in [6]) could be used to create a THz generator on the harmonics of the CR based on the inversion in crossed fields discussed. The cyclotron frequency harmonic amplification is well known in plasma physics and is used, for example, to explain the radio emission of the Sun.

The following steps to consider the discussed possibility of the CR amplification in graphene in strong E and crossed E, H fields — is the observation of reflection from a sandwich with an SLG or THz radiation passing through such a sandwich in a strong electric field in the SLG with or without a magnetic field.

Acknowledgments

The authors thank Eric Gornik (Vienna) for initiating this work.

Funding

The work was performed under the state contract of the IFM RAS No. 0030-2021-0020.

Conflict of interest

The authors declare that they have no conflict of interest.

References

[1] A.A. Andronov, V.A. Kozlov. JETP Lett., **17** (2), 124 (1973).
[2] A.A. Andronov, V.A. Kozlov, L.S. Mazov, V.N. Shastin. JETP Lett., **30** (9), 551 (1979).
[3] Yu.I. Ivanov, Yu.B. Vasiliev. Tech. Phys. Lett., **9** (10), 613 (1983).
[4] E. Gornik, A.A. Andronov. (eds *Infrared semiconductor lasers*) Optical and Quant. Electron., **23**, S1111 (1991).
[5] P. Pfeffer, P. Pfeffer, W. Zawadzki, K. Unterrainer, C. Kremser, C. Wurzer, E. Gornik, B. Murdin, C.R. Pidgeon. Phys. Rev. B, **47** (8), 4522 (1993).
[6] S. Boubanga-Tombet, D. Yadav, W. Knap, V.V. Popov, T. Otsuji. Phys. Rev. X, **10**, 031004 (2020). arXiv:1801, 04518 (2018).
[7] D.A. Bandurin, D. Svintsov, I. Gayduchenko, S.G. Xu, A. Principi, M. Moskotin, I. Tretyakov, D. Yagodkin, S. Zhukov, T. Taniguchi, K. Watanabe, I.V. Grigorieva, M. Polini, G.N. Goltzman, A.K. Geim, G. Fedorov. Nature Commun., **9**, 5392 (2018).

[8] D.A. Bandurin, E. Mönch, K. Kapralov, I.Y. Phinney, K. Linder, S. Liu, J.H. Edgar, I.A. Dmitriev, P. Jarillo-Herrero, D. Svintsov, S.D. Ganichev. Nature Phys., **18**, 462 (2022). https://doi.org/10.1038/s41567-021-01494-8
[9] M.A. Yamoah, W. Yang, E. Pop, D. Goldhaber-Gordon. ACS Nano, **11** (10), 9914 (2017).
[10] J. Chauhan, J. Guo. Appl. Phys. Lett., **95**, 023120 (2009).
[11] A.I. Berdyugin, N. Xin, H. Gao, S. Slizovskiy, Z. Dong, S. Bhattacharjee, P. Kumaravadivel, S. Xu, L.A. Ponomarenko, M. Holwill, D.A. Bandurin, M. Kim, Y. Cao, M.T. Greenaway, K.S. Novoselov, I.V. Grigorieva, K. Watanabe, T. Taniguchi, V.I. Fal'ko, L.S. Levitov, R.K. Kumar, A.K. Geim. Science, **375** (6579), 430 (2022).
[12] I.V. Oladyshkin, S.B. Bodrov, Y.A. Sergeev, A.I. Korytin, M.D. Tokman. Phys. Rev. B, **96** (15), 155401 (2017).
[13] A.A. Andronov, V.I. Pozdnyakova. Semiconductors, **54** (9), 1078 (2020).
[14] L.E. Vorobyev, S.N. Danilov, V.N. Tulupenko, D.A. Firsov. JETP Lett., **73** (5), 253 (2001).
[15] T. Fang, A. Konar, H. Xing, D. Jena. Phys. Rev. B, **84**, 125450 (2011).

Translated by A.Akhtyamov